JOURNAL OF GEOPHYSICAL RESEARCH, VOL. 104, NO. D24, PAGES 31,053–31,065, DECEMBER 27, 1999

Recording of El Niño in ice core $\delta^{18}O$ records from Nevado Huascarán, Peru

K. A. Henderson,[1] L. G. Thompson,[1] and P.-N. Lin

Byrd Polar Research Center, Ohio State University, Columbus

Abstract. The 68-year monthly resolved time series of $\delta^{18}O$ from ice cores retrieved from the glaciated col of Nevado Huascarán, Peru (9°S, 77°W, 6050 m) reflects climate variability over Amazonia and the western tropical Atlantic. Over the 25-year period (1968-1993) of midtroposphere observations, the interannual variations in Huascarán $\delta^{18}O$ relate closely with the zonal wind variations over tropical South America at the 500 hPa level. Additionally, there is some evidence that the spatial distribution of temperature anomalies in the western tropical Atlantic has influence on the 500 hPa circulation and hence the isotopic fractionation of moisture advected across Amazonia. During El Niño warming, the moisture convergence axis over the Atlantic Ocean is commonly diverted northward, leading to unusual warm and dry conditions over northeast Brazil, and ^{18}O-enriched snowfall at Huascarán. This enrichment phase is enhanced when the peak Pacific warming occurs during the first half of the calendar year, coincident with the wet season over Amazonia. Approximately 12 months later, the El Niño demise is affiliated with a reprisal of strong trade wind circulation, and the resultant cool, pluvial environment over Amazonia triggers a reversal to strongly depleted isotope anomalies.

1. Introduction

Oceanographers have known for several decades that temporary major redistributions of heat energy occur periodically in the surface waters of the tropical Pacific Ocean and that these events are innately linked with other unusual phenomena in and around the Pacific basin. This system, now referred to as the El Niño/Southern Oscillation (ENSO), includes both an atmospheric component and an oceanic component that are coupled so that variations in one fluid medium are simultaneously reflected in the other [*Enfield*, 1989]. Commonly seen teleconnections associated with El Niño include a strong Aleutian low, stronger extratropical westerlies and rainfall (along the sub-tropical jets), and droughts in northern Brazil, Australia, and Zimbabwe related to geographical shifts in convective activity [*Bjerknes*, 1969].

Our ability to provide forecasts of future ENSO activity, particularly in conjunction with recent warming, relies on the continued improvement of our understanding of the global climate system, as well as lengthening the temporal perspective of climate variability through the development of high-resolution paleoclimate records. To this end, two ice cores to bedrock were extracted from the glaciated col of Nevado Huascarán, Peru (Figure 1) in the chain of Andean Mountains known as the Cordillera Blanca. The ice thickness in the center of the col is 160-165 m and is a continuous archive of snowfall covering the past 15,000 to 20,000 years [*Thompson et al.*, 1995]. Because yearly snow accumulation is presently 1.4-1.8 m H_2O eq, annual layer thicknesses for the top 100 years remain sufficiently large for extracting highly detailed records. With very little seasonal melting and near-absolute dating for much of this time period, the Huascarán ice cores constitute a high-resolution proxy record of environmental conditions within the realm of the ENSO phenomenon.

Despite the close proximity of Huascarán to the Pacific Ocean, the persistence of easterlies determines the moisture source for Andean precipitation to be predominately Atlantic-derived [*Johnson*, 1976]. Whereas ENSO is primarily a Pacific basin phenomenon, Atlantic sea surface temperatures (SSTs) often reflect the warming/cooling events in the tropical Pacific lagged by six to eight months. The SST anomalies in the tropical Atlantic are substantially weaker than those observed in the equatorial Pacific in association with ENSO [*Wallace et al.*, 1998], of the order of 0.8°-1.2°C in the equatorial Atlantic compared to 3°-5°C for strong coastal Pacific warming. According to basic isotopic fractionation theory [*Jouzel*, 1986], this small range of interannual variation alone should not act as the controlling factor on the resultant isotopic composition of atmospheric water vapor or condensate over inland sites in South America. However, it remains possible that some fluctuations in the Atlantic sector are enhanced through tropical atmospheric processes, such as low-level convergence within the Intertropical Convergence Zone (ITCZ) and over the Amazon Basin. A mechanism by which Pacific anomalies can be transferred (or teleconnected) to the Atlantic Basin has been described as a "tropical atmospheric bridge" by *Klein et al.* [1999]. They postulate that during El Niño the net heat flux entering the tropical Atlantic is enhanced by a reduction in cloud cover and evaporation in response to a weakened Hadley circulation. In this

[1]Byrd Polar Research Center and Department of Geological Sciences, Ohio State University, Columbus, Ohio.

Paper number 1999JD900966.
0148-0227/99/1999JD900966$09.00

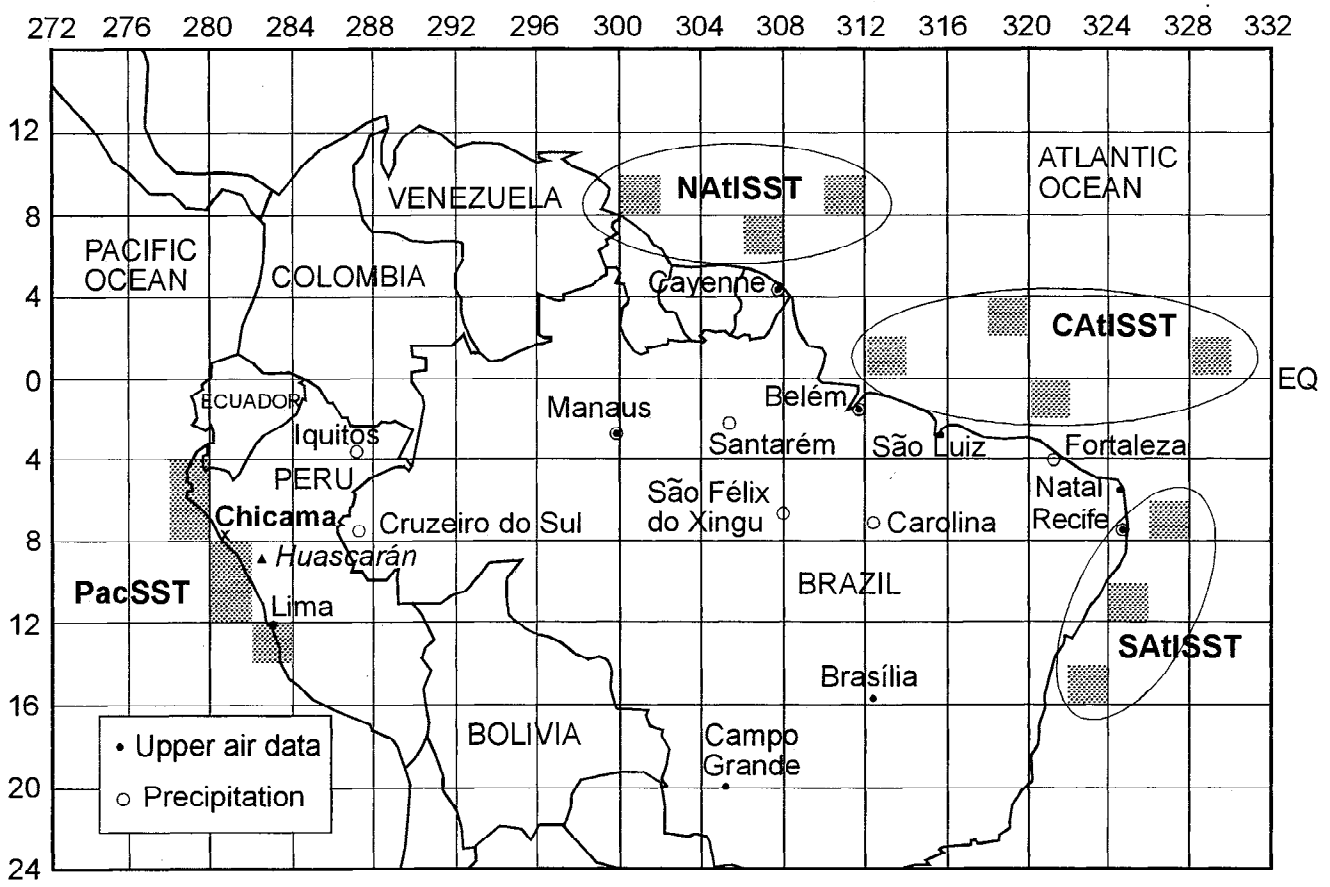

Figure 1. Map showing the position of Nevado Huascarán, and the location of COADS/ds277.0 grid boxes (shaded) used for creation of PacSST (left), and the three subregions (north, central, and south) combined to produce the AtlSST time series (right). The coastal SST monitoring station (Puerto de Chicama, Peru) is indicated in boldface. Also shown are the locations of ten/nine meteorological stations for which precipitation/upper air data were compiled to create the various tropical South American indices.

way the nodal pressure boundary which runs generally along the Andean range defines an additional cell component of the east-west Pacific Walker circulation [*Webster*, 1983].

In ice core research, many different measurements can be applicable to various local and regional environmental conditions. For example, a visual ice core-stratigraphic record produced from the Quelccaya Ice Cap, Peru (14°S, 71°W, 5670 m), showed a 30% accumulation decrease during recent El Niño years [*Thompson et al.*, 1984b]. However, for this study the record of oxygen isotopic composition ($\delta^{18}O$) from Huascarán was the main focus, as it is subannually resolved, and potentially reflects the temperature and precipitation history of air masses propagating westward from the tropical Atlantic across most of tropical South America. (Interestingly, the Huascarán accumulation history showed little relationship with either ENSO or the Quelccaya data [*Henderson*, 1996], suggesting significant local control on precipitation at this more equatorial site). The absence of any easily visible 4- to 5-year periodicity in the Huascarán isotopic record (Figure 2) indicates the lack of any consistent first-order control by Pacific (or Atlantic) SSTs. Hence the Huascarán isotope time series is not a true ENSO paleorecord in itself (correlations are negligible even calculated from annual averages), though it remained possible to define the characteristic isotopic response to both El Niños and cold events and to compare the two.

Bradley et al. [1987] performed a superposed epoch analysis (SEA) on continental air temperatures at various latitude bands in the tropics and subtropics of the Northern Hemisphere. On the basis of an invariant "zero" month (April of year 0, using the chronology provided by *Rasmusson and Carpenter* [1982]), six-year epochs of monthly anomalies from individual stations were superposed and summed (i.e., stacked), creating composite signatures for warm and cold events. In similar fashion, the characteristic response in Huascarán $\delta^{18}O$ to ENSO events was determined by treating each as an individual episode centered on the timing of the peak SST anomaly along coastal Peru. Variations in the timing of peak Pacific warming (or cooling) provided the basis for comparing the ice core-isotopic response to early (January-July peak) and late (August-December peak) events.

Special attention was given to the most recent 25-year period, for which additional observations of middle and upper tropospheric conditions are available over limited areas of South America. These additional data made possible a more in-depth examination of the relationship among $\delta^{18}O$ and temperature, humidity, precipitation, and atmospheric circulation. Tropical meteoric water reservoirs do not undergo isotopic fractionation in a manner that yields a positive linear relationship to air temperature, such as what occurs at higher latitudes [*Grootes et al.*, 1989; *Yao et al.*, 1996; *Rozanski et al.*, 1997]. Accordingly, the competing effects of temperature, precipitation, and circulation on the resulting isotopic composition of Andean precipitation must be evaluated, and over progressively longer time windows. Once quantifiable relationships are developed, the

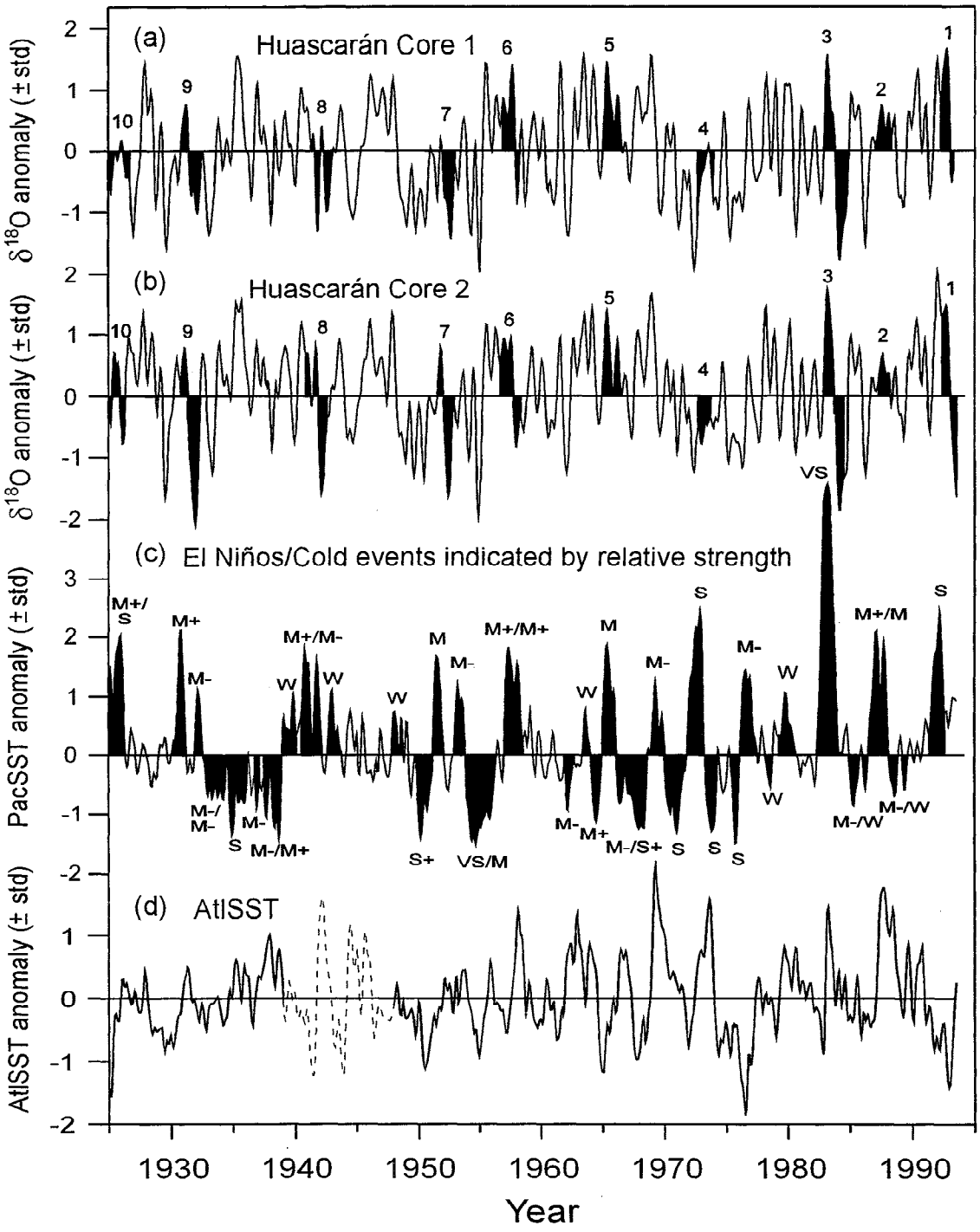

Figure 2. Comparison of the $\delta^{18}O$ anomaly records from (a) HSC1 and (b) HSC2, both filtered with a seven-point "cosine-bell" function (7SRMcb), and (c) the PacSST anomaly record for coastal Peru (derived from COADS/ds277.0/Chicama), 5SRMcb, for the period 1925-1993. Numbered and shaded intervals in Figures 2a and 2b depict the individual "lee" responses to the 10 largest El Niños. Letter designations in Figure 2c represent relative magnitudes of identified El Niños and cold events. For Figures 2c and 2d the enhanced late 20th century warming in the COADS data [*Folland and Parker*, 1995], due to a sudden change from the use of canvas or wooden buckets to engine intake thermometers in the early 1940s, was removed by adding 0.5°C (based on *Kaplan et al.* [1998]) to all COADS SSTs before January 1940. This correction was allowed to decay in 0.01°C increments (per month), reaching zero at February 1944.

physical mechanisms by which strong Pacific events are manifested as climatic shifts in the source region for Andean moisture can be identified much more convincingly. In section 4, a schematic is presented that diagrams a potential sequence of anomalous events associated with a "canonical" El Niño that may result in the signature in Huascarán $\delta^{18}O$ and available meteorological data.

2. Data and Methodology

2.1. Site Description and Analysis

In July-August 1993, two ice cores to bedrock were recovered from the col between the north and south peaks of Nevado Huascarán, Peru (9°S, 77°30'W, col elevation 6050 m) (Figure 1) and were subsequently transported back to the cold room facility at the Byrd Polar Research Center (BPRC). Core 1 (HSC1, 160.40 m) was sectioned in the field into 2677 samples decreasing in thickness from 13 cm at the top to 3 cm at the base, which were then melted and poured into 2 or 4 oz. plastic (HDPE) bottles and sealed with wax. Core 2 (HSC2, 166.08 m), drilled approximately 100 m from the HSC1 site, was returned frozen in 1 m sections. Ice motion vectors determined from stake movements from 1991 to 1993 indicate that the drill sites are proximal to the divide between ice flow toward the east and west outlets of the col. Visible observations and borehole temperatures indicate that the glacier is "polar" type; that is, it remains frozen to the bed [*Thompson et al.*, 1995].

Each ice sample from HSC2 was prepared in a Class 100 clean room environment and analyzed for major anion concentrations (Cl^-, NO_3^-, and SO_4^{2-}) on a Dionex 2010i ion chromatograph, $\delta^{18}O$ on a Finnigan Mat mass spectrometer [*Craig*, 1957], and for particulate concentration and size distribution using a Coulter TA-II particle counter [*Thompson*, 1973]. A complete $\delta^{18}O$ profile was also produced from the bottled samples from HSC1. Contamination during field preparation and transport of these samples precluded the development of a second complete record of particles and anion concentrations.

2.2. Development of the Time/Depth Relationship

Tropical South American climate is marked by annual dry seasons (July-October) which were identifiable in the Huascarán ice core record as elevated values in all relevant measurements. (Occurrence of ice layers in the Huascarán core is subject to multiple dry seasons in some years and does not yield an accurate dating tool.) The nitrate (NO_3^-) record provided the most definitive seasonal marker, but the final timescale was constructed from a comparison of four major parameters [*Thompson et al.*, 1995]. Each annual maximum corresponds to the middle of the dry season, assumed to occur on the August 1. The rapid layer-thinning below 120 m limited annual resolution to the most recent 270 years. However, the high accumulation and strong preservation of seasonal cycles also made possible the subannual resolution of $\delta^{18}O$ variations for a period of 110 years (1884-1993).

The accuracy of the timescale is of paramount importance in the development of relationships between ice core proxy data and tropical climate conditions. Several horizons in recent times confirmed the layer counting as a reliable method and indicate almost certain ages for the uppermost 50 years. In 1980, during the original reconnaissance expedition to Huascarán, a 10 m firn core was extracted and analyzed for $\delta^{18}O$ at BPRC [*Thompson et al.*, 1984a]. Aside from minor accumulation variation and slight signal attenuation, the 1993 cores duplicated the earlier stable isotope profile over the common portion and confirmed the layer counting to 1980 as absolute. Additionally, a magnitude 7.7 earthquake struck coastal Peru in May 1970, generating large mud flows following the collapse of a large portion of the Huascarán glacier from the north peak. The event was recognized in the ice core by a sharp 2-year rise in particulates from the newly created sediment source. A third time horizon was provided by the HSC2 ^{36}Cl profile [*Synal et al.*, 1997], a substance produced by neutron activation during the explosion of atomic devices in the presence of a ^{35}Cl source, such as sea water. An abrupt >100-fold rise in ^{36}Cl concentration occurred at ~54-m depth, which dates (by layer counting) to 1951-1953. This was in direct response to the October 31, 1952, U.S. "Ivy" surface test of an experimental nuclear device on the Eniwetok Atoll in the Pacific Ocean (11°N, 162°E) [*Carter and Moghissi*, 1977]. Finally, in both HSC1 and HSC2 the 1883 eruption of Krakatau, Indonesia (6°S, 105°30'E) was identified by an anomalous sulfate concentration of ~400 ppb at 110-m depth, more than twice the level of any other local (within 10 m) event. A date of midyear 1884 was thus considered to be an absolute time marker for both cores within the error of the time lag (less than 1 year).

2.3. Preparation of the Ice Core and Climatological Data Sets

The high accumulation on Huascarán provided a sample density (defined as the number of core segments cut per year of accumulation) sufficient to retain monthly resolution for 110 years, although because of temporal uncertainties in the earlier portion, only the most recent 68 years were analyzed. To facilitate comparisons between ice core parameters and climatological data sets, the Huascarán records were transferred to a timescale with a constant interval. This "time-linearizing" technique involved dividing each "thermal" year (August 1 to subsequent July 31) into 12 separate bins of equal thickness (or depth) to yield a continuous "quasi-monthly" time series. Certainly, the complex interaction of varying accumulation rates within a year, sampling intervals, averaging techniques, and indefinite dry season time horizons are all potential errors when compared to real time. Dividing the annual oxygen isotope record into 12 monthly increments was justified because the annual oxygen isotopic signal preserved in the ice core is remarkably evenly proportioned between enriched (dry season) and depleted (wet season) isotopic values. The reasons for this are at least twofold: first, during the dry season it seldom rains at lower elevations; however, often clouds will form on the mountain tops and snow will fall on these high-elevation snowfields. Second, work in the polar regions [e.g., *Hammer et al.*, 1978] has proven that the isotopic input signal from individual snow events is much noisier than the record preserved in the snowpack. The mass exchange by diffusion via the vapor phase in the porous snow usually obliterates the high-frequency variability in $\delta^{18}O$ within a few years, depending on the temperature and the thickness of the individual layers. Furthermore, sublimation enrichment [*Grootes et al.*, 1989] of near-surface late-winter snowfall may also contribute to an increased representation by ^{18}O-enriched snowfall. Thus the dry season $\delta^{18}O$ signal is distributed over a greater percentage of each annual increment than might be expected from the annual precipitation patterns observed at the lower-elevation meteorological stations.

Within each year, each measured $\delta^{18}O$ value was funneled into the monthly bin corresponding to the sample depth. A large majority of years did not fortuitously have exactly 12 measurements, so adjustments were required. Those years with fewer samples required the insertion of simple averages of the two

measurements on either side of each previously empty bin. In contrast, years with sample density (x) greater than 12 normally produced (x - 12) values that were averages of two measurements, up to x = 24. Only three years had more than 24 samples and required averages of three values. For HSC2, a total of 978 samples covered the 823 months that were time-linearized. In summary, 566 (68.8%) of the 823 months represented an unmodified value transferred to the timescale, 200 (24.3%) represented an average of two values within a bin, 4 (0.5%) represented three values, and the remaining 53 (6.4%) were interpolated values.

The identical procedure was performed for the second core, HSC1, and confirmed that this procedure truly captured the temporal fluctuations in the Huascarán $\delta^{18}O$ record. For the 820 months (the top three months of accumulation were lost in the drilling) covering the top 68 years of HSC1, only 810 samples were cut; 596 months (72.7%) were single measurements; 104 (12.7%) were averages of two samples; 2 (0.1%) were averages of three; and 118 (14.4%) were interpolated values. Although HSC1 was sampled more coarsely, the major subannual and interannual variations were duplicated (Figure 2a), yielding particularly good correlations over the last 40 years. Because HSC1 lacks monthly resolution before 1940, HSC2 should be considered to be the superior temporally resolved record.

For the identical period (1925-1993), monthly averaged SST anomaly data sets were created for both the tropical Pacific and Atlantic oceans (Figure 1) in the regions that might influence the isotopic composition of Huascarán snowfall. Although SST anomalies are readily available for various regions of the tropical Pacific (e.g., Niño 1+2 and Niño 3), these indices have not been extended back beyond 1950 and thus were insufficient for this analysis. Furthermore, the SST time series recently produced by *Kaplan et al.* [1998] did not include Niño 1+2 (the area of particular interest here), which exhibits a variable lead of 0-5 months relative to Niño 3.

Since World War II (WWII) interrupted the commercial and research ship traffic over much of this region resulting in sparse data collection, data from several sources and various locations were combined to circumvent any gaps. For coastal Peru (Pacific SST data set, abbreviated PacSST), the following products were employed: (1) Coupled Ocean-Atmosphere Data Set (COADS) Monthly Summary Trimmed Groups (MSTG) Group 3 subset (1925-1979) - global 2° x 2° grid [*Woodruff et al.*, 1987]; (2) National Center for Atmospheric Research (NCAR) ds277.0 "recon" SST data set, filtered by EOF analysis (1950-1992) - COADS grid; and (3) Puerto de Chicama, Peru (7°42'S, 79°27'W) coastal data set (1925-1992) [*Quispe Arce*, 1993]. Because all three of the data sets span the period from 1950 to 1980 all SST anomalies were determined with respect to this common period. On the basis of the COADS grid, data from five coastal grid boxes (Figure 1), incorporating also the entire Puerto de Chicama time series (continuous through WWII), were used to construct the PacSST data set. Each monthly value was a simple arithmetic mean of all anomaly values (up to six) available. The final construction of the PacSST anomaly time series (Figure 2c) involved piecing together the COADS and ds277.0 profiles, linked by their common climatology. For the period from 1950 to 1979 in the final PacSST record, the ds277.0 "recon" anomalies were selected because of the posttreatment.

The methodology for creating the SST anomaly datasets of the western tropical Atlantic was similar to that used for PacSST. However, because both mean SSTs and the meridional SST gradient have both been shown to have influence on the climate of Brazil [*Servain*, 1991; *Uvo et al.*, 1998], grid points were chosen on the basis of both data continuity and spatial coverage, intending to illustrate SST patterns. Therefore coastal Atlantic SSTs were averaged for three separate regions, off the coast from the Guianas (NAtlSST), the Nordeste region (CAtlSST), and east central Brazil (SAtlSST). The composite AtlSST index (Figure 2d) represents a simple arithmetic mean of the three regional anomaly time series. Given the sparseness of available data during WWII, AtlSST values for the years 1939-1947 were eliminated from future superposed epoch analysis (SEA) composites.

Monthly averaged surface and upper air data for many tropical South American locations (Figure 1) were extracted from the journal *Monthly Climatic Data for the World* for 1968 through 1993. Temperature, wind vectors, dew point, and geopotential height data were gathered for nine sites at each of the standard levels of the lower and midtroposphere (850, 700, and 500 hPa). Surface data compiled included temperature, pressure, dew point, and precipitation (10 separate sites, confined to Amazonia). For certain years the reporting of data was sporadic, so the individual records were combined into single time series that encompass the entire region surrounding the Amazon Basin. Long-term monthly means were determined using the entire length of the individual records as the basis for the climatology. Anomalies were usually not standardized in this case, as the standard deviations were often suspect due to the poor continuity of some of the records. For each pressure level, the anomaly records followed a standard nomenclature: for example, "SA-850t" represents the temperature anomaly time series at the 850 hPa level averaged over all nine sites, unless otherwise stated. Other abbreviations used include u=zonal wind and k=atmospheric thickness.

3. Results

3.1. Superposed Epoch Analysis

The timing, spatial extent, and relative strength of El Niño events are well known for the past 100 years, although this historical record differs with the choice of the various indices (both climatological and phenological) which are directly (or indirectly) responsive to the ENSO phenomenon. One such El Niño record was developed by *Quinn* [1993], and covers the time period from 1525 to the present. This reconstruction was based not only on sea surface and air temperatures but also recorded episodic events like incidents of flood damage, mass mortality or migration of sea life, and travel-time variations for commercial vessels. Because only the absolute oceanographic conditions should influence the geochemistry of high Andean snowfall, it was deemed more appropriate to create a separate El Niño record based solely on the PacSST time series.

The method for classifying ENSO events was necessarily subjective to a degree, as maximum warming/cooling, duration of sustained anomalous conditions, and the peak characteristics (e.g., single versus double) were all considered. The use (and overall frequency) of the letter designations VS, S+, S, M+, M, and M- was retained from the Quinn analysis, and a weak (W) classification was added for borderline anomalies. These designations were applied also to cold events in an analogous way. Those events, which displayed two distinct maxima/minima separated by a significant length of time, were classified as "2-year" events. Although no specific period between peaks was strictly set, most successive peaks of 2-year events were separated by 10 to 16 months. Unlike Quinn's analysis, each of the multiple peaks were given a separate magnitude rating, and the response of the ice core record was considered for each maximum or minimum. A total of 19 El Niño events (four 2-year events)

were identified in the PacSST analysis (Table 1), compared to 16 identified by Quinn. Only a few events failed to be identified in each record (none of these being strong events), with the level of agreement generally improving through time toward the present. A total of 15 cold events (six 2-year events) were denoted in the PacSST analysis.

Following the superposed epoch analysis (SEA) procedure of *Bradley et al.* [1987], SST and $\delta^{18}O$ anomalies were superposed and averaged for a period beginning 36 months before and ending 36 months after the identified zero month (in this case, the midpoint of each coastal Pacific (PacSST) warming). The 73-month SEA composites of PacSST and HSC2 $\delta^{18}O$ anomalies for all El Niño and cold events are depicted in Figures 3a and 3b. Indicated also on the HSC2 $\delta^{18}O$ graph (dotted lines) is the 95% confidence interval based on a Monte Carlo analysis involving 400 simulations of 22 (the average number of warm/cold events) randomly selected and superposed epochs [*Bradley et al.*, 1987]. In the "lee" 16 months following the peak PacSST anomaly there appears evidence for an ENSO signature in the Huascarán $\delta^{18}O$ composite. In the El Niño (cold event) case, the SEA results demonstrate above- (below) normal values for ~6 to 8 months after the zero month, followed by a longer period (~10 months) of below- (above) normal values. Also evident is an enrichment (depletion) of ^{18}O during warm (cold) phases ~18-20 months preceding the peak anomaly.

To further investigate the characteristics of this isotopic ENSO signal, a change was made to the SEA procedure in order to eliminate complicating phenomena. First, the weaker events were filtered out to accentuate the response to stronger events, i.e., those more likely to influence Andean precipitation. Also, the secondary maxima (or minima) for 2-year events were eliminated from the composite except for two cold events (1938 and 1968) when the later peak was retained, because each was two (or more) grade levels higher than the initial peak phase. The ENSO events of this subset are shown in italics in Table 1 and numbered sequentially in Figures 2a and 2b; the resultant SEA profiles are shown in Figure 3c. The characteristics of the lee responses to warm and cold events are generally unchanged and remain strongly anticorrelated. However, the oscillations in both cases have become stronger once the minor events and complicating factors were removed. Also, the distribution of anomalies in other parts of the 73-month window remain nearly random (with the exception again of the 19-month periodicity), indicating that the HSC2 response to PacSST anomalies begins only after the ENSO event has reached peak level.

Table 1. Listing of Identified El Niño and Cold Events Derived From PacSST Anomalies

El Niños		Cold Events	
Center Month	Strength	Center Month	Strength
3/1992	S	5/1989	W
10/1987	M	9/1988	M-
3/1987	M	4/1986	W
2/1983	VS	5/1985	M-
10/1979	W	8/1978	W
8/1976	M-	*11/1975*	S
10/1972	S	*11/1973*	S
5/1969	M-	*1/1971*	S
7/1965	M	*1/1968*	S+
9/1963	W	6/1966	M-
2/1958	M+	*7/1964*	M+
5/1957	M+	3/1962	M-
6/1953	M-	11/1955	M
8/1951	M+	*10/1954*	VS
9/1948	W	*4/1950*	S+
1/1943	W	*8/1938*	M+
11/1941	M-	10/1937	M-
1/1941	M+	12/1936	M-
11/1939	W	*12/1934*	S
4/1932	M-	10/1933	M-
11/1930	M+	12/1932	W
12/1925	S		
3/1925	M+		

VS, very strong; S, strong; M, medium; W, weak.

El Niño SEA composites of PacSST, AtlSST, N-S AtlSST gradient, and HSC2 $\delta^{18}O$ were also generated according to peak PacSST timing, i.e,. early (January-July) versus late (August-December) events (again, only magnitude M or greater). The results, simplified by a smoothing function and including only the central 33-month portion, are displayed in Figure 4. The lee-wave response in HSC2 $\delta^{18}O$ appears more distinct in the early composite, due mainly to the strong enrichment phase centered on month "zero" that is muted over the five late events. (As before, the composite responses of HSC2 $\delta^{18}O$ to cold events (not shown) mirrors that of the warm events from 0 to +16 months.) Also observed is a difference in the phase relationship between PacSST and AtlSST, as the onset of western Atlantic warming in the early case occurs only after coastal Peru temperatures have reached their maximum. AtlSST warming begins sooner (6-8 months before the PacSST peak) in the late composite. A similar phase shift is seen between the respective composites of the N-S AtlSST gradient, such that significant northward shifts in SST occur in the lee phase (0 to +16 months) only for the early composite.

The simple differencing of the NAtlSST and SAtlSST anomaly data sets provided a measure of the meridional heat distribution across the moisture source region for Huascarán precipitation and is comparable to the "dipole index" as defined by *Servain* [1991]. *Hastenrath* [1978] showed that a typical pattern of tropical Atlantic SST anomalies exists (warm off the coast of Angola and cold near the Caribbean) during times when the ITCZ is positioned anomalously far south (a condition often coincident with the cold phase of ENSO). This pattern has then been identified as a cause of high rainfall events in the Ceará region of Brazil, the antithesis being the major droughts (sêcas) which occur there coincident with the stronger Pacific warm events. A series of more recent studies [*Mehta and Delworth*, 1995; *Carton et al.*, 1996; *Chang et al.*, 1997; *Mehta*, 1998; *Xie*, 1999] confirm this relationship and point to a decadal oscillation in addition to the relationship with ENSO. However, *Houghton and Tourre* [1992] have argued that the decadal nature of the meridional gradient is more accurately two independent modes acting separately north and south of the equator rather than as a true dipole.

3.2. Relationship Between Huascarán $\delta^{18}O$ and Tropical Meteorology

In section 3.1, the characteristic ENSO signal in the isotopic composition of archived snowfall in the col of Nevado Huascarán was identified and illustrated. For the purpose of identifying a potential mechanism by which anomalous Pacific SSTs could influence high Andean isotope values, it is useful to examine the relationship between the interannual variability in HSC2 isotopic composition and the conditions of the tropical atmosphere (Figure 5). Thus the time series of the various climatological variables available at the surface and at the 850, 700, and 500 hPa levels were compared with the HSC1/2 $\delta^{18}O$ anomaly time series. The only significant covariance ($R^2 = 0.30$ for the period 1973-1993, averaged quarterly) between the ice core $\delta^{18}O$ (Figure 5c) and the

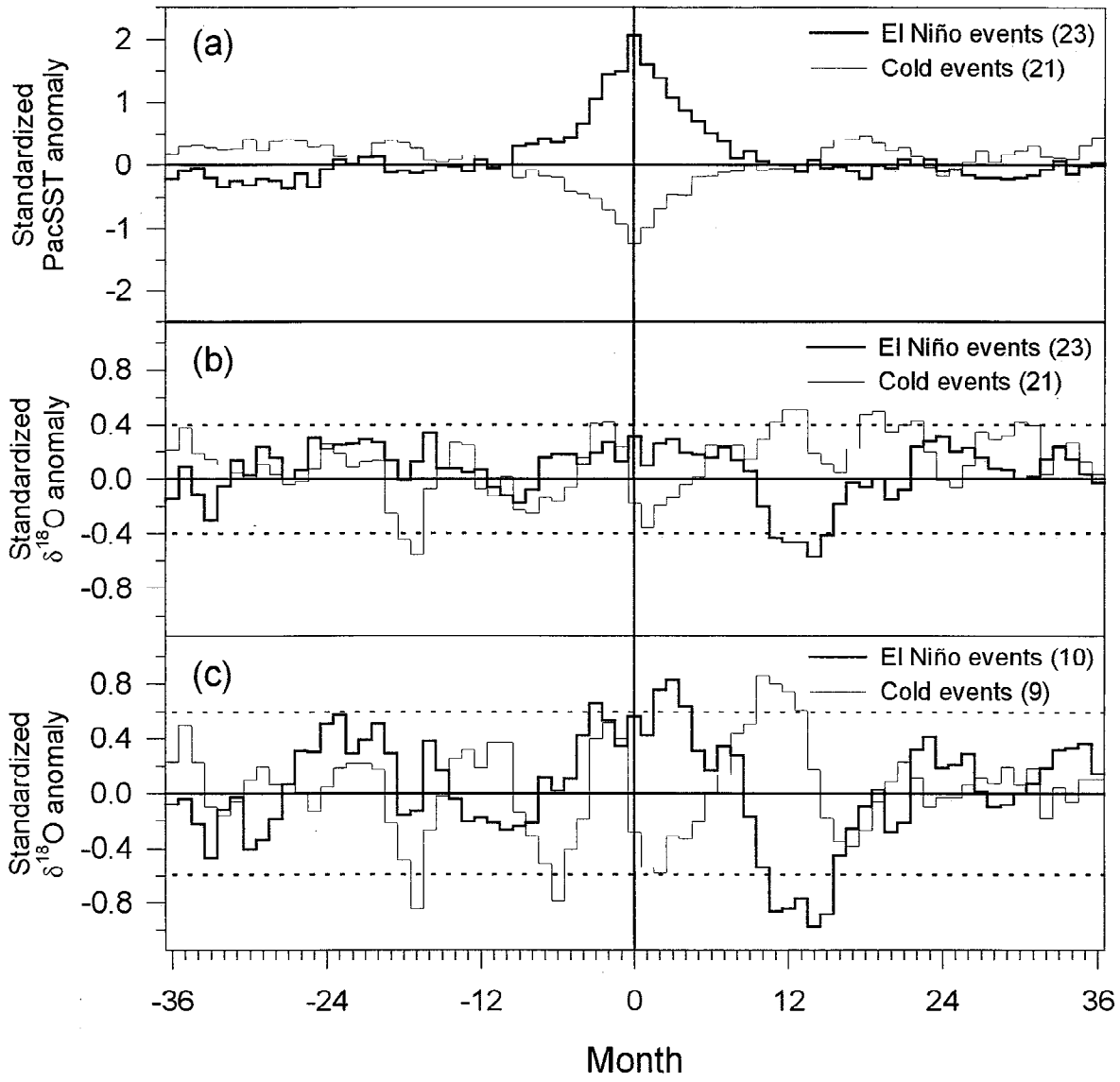

Figure 3. Superposed epoch analysis results (1925-1993) for (a) PacSST and (b) Huascarán $\delta^{18}O$ anomalies, both including all identified warm and cold events, and (c) Huascarán $\delta^{18}O$, but only for events with magnitude M or greater, and including only one epoch per each 2-year event. Dotted lines (in Figure 3b and 3c) indicate the 95% confidence interval based on 400 Monte Carlo simulations.

meteorological data is with the zonal wind velocity anomalies at 500 hPa (Figure 5b). Interestingly, the lower-level zonal winds (Figure 5a) display a greatly different behavior over this 25-year period and no clear relationship with either the winds aloft or the Huascarán record. Also, because rainfall (Figure 5d, inverted), temperature/thickness (Figure 5f), humidity, and pressure (not shown) anomalies also lack any significant covariance with the ice core $\delta^{18}O$, it puts into question whether the short-term variations in isotopic composition are recording regional climate in a recognizable fashion.

Rayleigh fractionation theory [*Jouzel*, 1986] has proven useful in providing a physical link between the water vapor budgets necessary for isotopic depletion and the surface atmospheric temperatures over high-latitude ice caps [*Dansgaard et al.*, 1973]. While the exact transfer functions have come under some scrutiny [*Cuffey et al.*, 1995], especially under different climate regimes of the past, the temperature-$\delta^{18}O$ relationship in high-latitude environments has been empirically shown to have a consistent (positive) linear relationship [*Johnsen et al.*, 1989]. In the case of a tropical ice cap such as Huascarán, the seasonal $\delta^{18}O$-T relationship is actually reverse of that found at higher latitudes; that is, the most depleted values occur in the warmest times of the year. A modeling study by *Grootes et al.* [1989] which involved the basin hydrology of Amazonia as a controlling mechanism on the Rayleigh "f" parameter ("water vapor fraction remaining") detailed how a reverse relationship is possible.

While these attempts at connecting physical mechanisms to the seasonal cycle in tropical meteorology are pertinent to the application of geochemical measurements as climatological proxies, as of yet the processes responsible for the interannual isotopic variability (i.e., the $\delta^{18}O$ anomalies as in Figure 2) are not sufficiently established. However, it is readily apparent that the century-scale to millennial-scale isotopic fluctuations in Andean cores are primarily temperature-dependent in a similar manner as in higher latitudes, i.e., a positive relationship. Well-documented recent events such as the Little Ice Age and 20th century warming

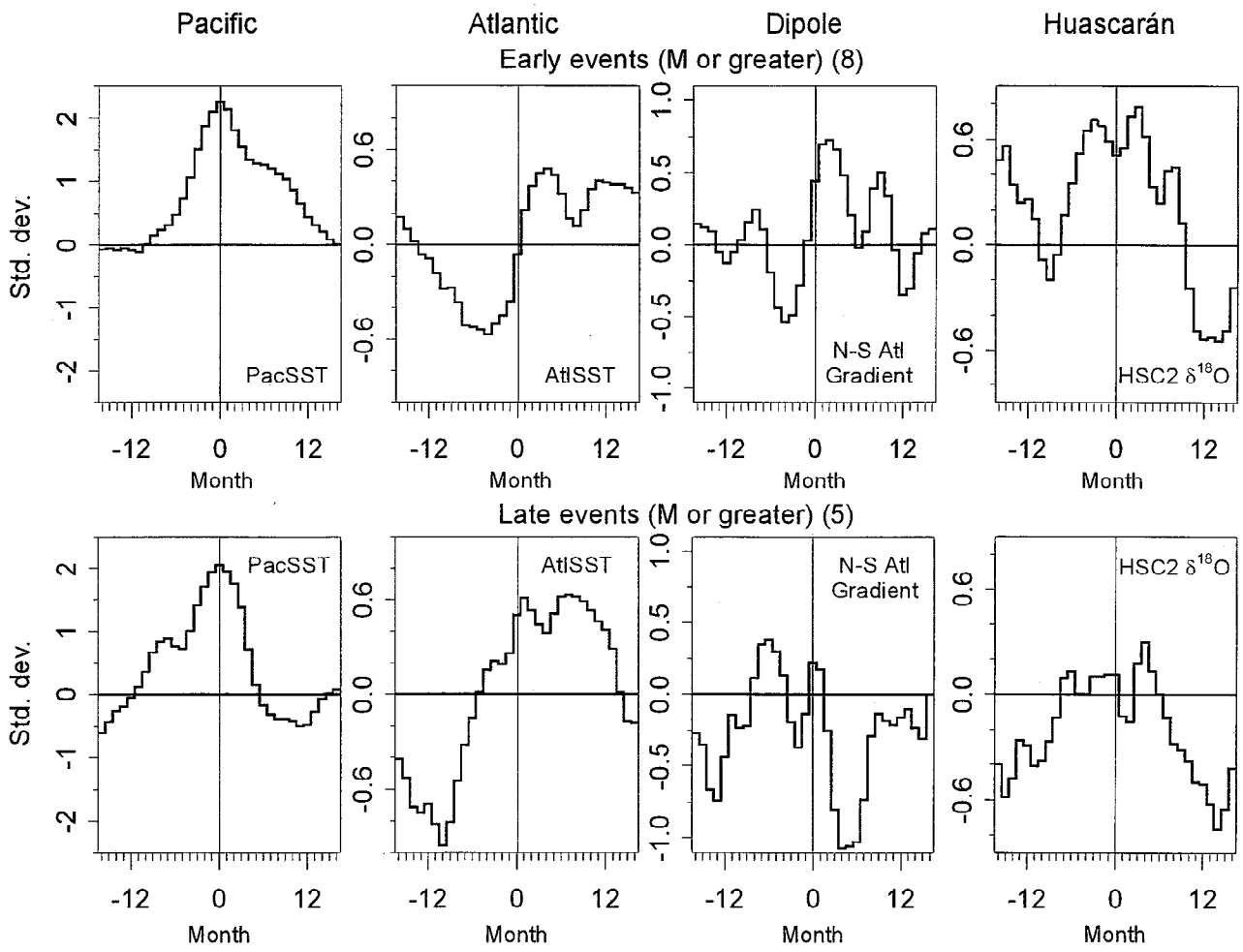

Figure 4. The 33-month SEA composites (1-2-1 filtered) of the various responses to El Niño events (M or greater), according to the timing of peak Pacific warming (1925-1993). Early events (January-July peak) (top); late events (August-December peak) (bottom).

[*Thompson et al.*, 1993] impart strong evidence for this conclusion, but even stronger validation lies in the 5-6‰ shift across the glacial-interglacial transition and the identification of a Younger-Dryas signature in both the Huascarán [*Thompson et al.*, 1995] and the Sajama, Bolivia [*Thompson et al.*, 1998] ice cores. The following question remains: If stationary surface temperature is to be the chosen proxied parameter, at what temporal window length does the tropical $\delta^{18}O$-T relationship become reversed?

Furthermore, because the interannual HSC2 $\delta^{18}O$ lacks correlation with tropical climate observations (with the exception of the midtroposphere zonal winds), it questions whether most time-averaged conditions are applicable to an archive of episodic events, such as in an alpine ice cap [*Vuille et al.*, 1998]. Also, because the air at 500 hPa carries so little water vapor and because wind velocity alone can scarcely be considered an agent of Rayleigh fractionation, it is difficult to reconcile this isolated relationship with known physical processes. However, since wind velocities at 500 hPa are generally dependent upon the meridional temperature gradient, one might expect to see a relation between the ice core variations and the north-south SST patterns along the east coast of tropical South America. For this reason the N-S AtlSST difference profile is also included in Figure 5e. In fact, some similar variations are seen, particularly on a multiyear basis, with northward thermal shifts being coincident with weak easterlies and also ^{18}O-enriched snowfall at Huascarán.

Considering the entire 25-year period, the two distinct minima (around 1974 and 1985) in the N-S AtlSST gradient may be a manifestation of the near-decadal oscillation previously noted, though it is not particularly obvious in earlier decades (e.g., 1950s and 1960s). However, a recent statistical study of the Atlantic dipole [*Mehta*, 1998] found that the strongest decadal oscillation (12- to 13-year period) occurs in the South Atlantic centered at 15°S, 5°E (far east of SAtlSST) and that the behavior is regular and consistent throughout the 20th century. Furthermore, a strong covariance (~0.9) between the dipole behavior and the analogous oscillation in Nordeste precipitation was identified for the period 1912-1985. In Figures 5b-5d there is also a less distinct in-phase decadal character evident in the 500 hPa zonal winds and ice core $\delta^{18}O$ records. In fact, the leading pair of eigenvalues determined from singular-spectrum analysis [*Vautard et al.*, 1992] of either HSC1 or HSC2 $\delta^{18}O$ is a regular oscillation with a mean period of 10.8 years which retains a consistent amplitude through the 20th century [*Henderson*, 1996]. The Quelccaya ice core $\delta^{18}O$ record [*Thompson*, 1992], although lacking the high resolution of the HSC2 core, displays a nearly identical decadal oscillation that remains in phase for at least the last 100 years (when dating

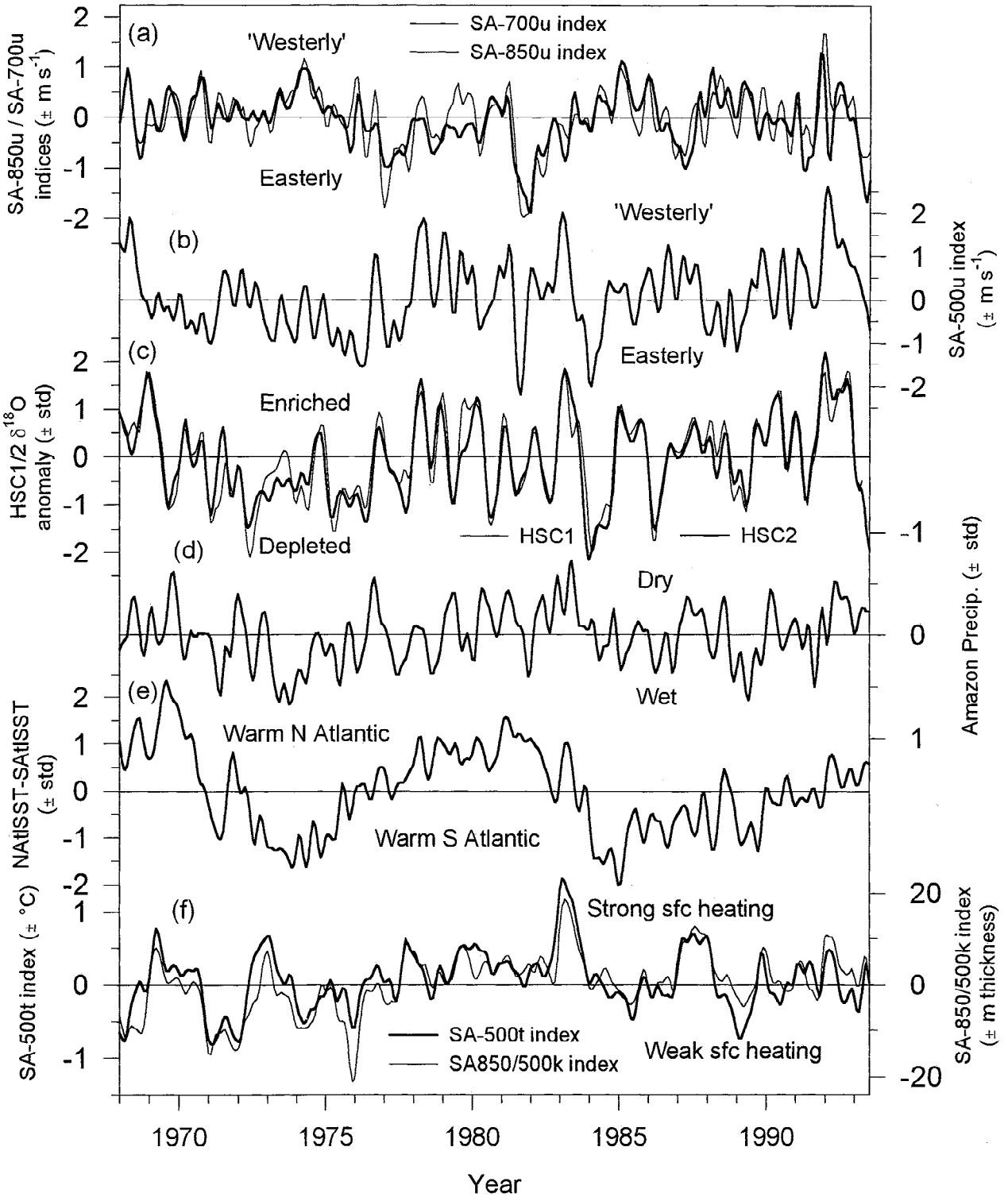

Figure 5. Comparison of (a) SA-850u and SA-700u indices, (b) SA-500u index, (c) HSC2 $\delta^{18}O$ anomalies, (d) Amazon precipitation anomalies, (e) N-S AtlSST gradient, and (f) SA-850/500k (thickness) and SA-500t indices, all as 5SRMcb (1-3-4-3-1 filter). For indices shown in Figure 5f, only the six northeastern sites (dots in Figure 1) were used.

accuracy for both is nearly certain). In the end, there appears a similarity in the relationships between tropical SST patterns and resultant climatic responses in the interior of South America, for both ENSO and decadal-scale variability and over significant lengths of time (100 years or more).

4. Discussion

Following superposed epoch analysis the characteristic ENSO signal in the Huascarán ice core record is a roughly symmetrical wave in the $\delta^{18}O$ anomaly profiles, with a peak nearly coincident

with the maximum/minimum PacSST and an opposite peak in the composite roughly 12 months afterward. Despite the poorer resolution the SEA composites of HSC1 (not shown) are very similar and attain nearly the same level of significance as for HSC2, indicating reproducibility. Using the HSC2 lee wave as a paradigm for estimating the influence of individual ENSO events on the Atlantic/Amazon climate regime, the conclusion can be made that the influence of the El Niño events of 1992, 1983, 1952, 1941, and 1930 was strong (Figures 2a and 2b). In contrast, the 1987, 1972, and 1965 events generated only a weak or negligible influence, whereas the remaining two (1925 and 1957) were intermediate. Because this pattern of responses is generally opposite to the nature of the El Niño-related AtlSST warmings (seen in Figure 2d), it raises the possibility that the contrast between equatorial SST anomalies on either side of the South American continent is of major importance to the occurrence of well-defined oscillations in the ice core $\delta^{18}O$ and by association, perhaps precipitation and circulation anomalies over Amazonia as a whole.

The lack of any relationship between the composite warm and cold signals in the 8 months preceding the maximum, i.e., during anomaly growth, indicates that the Huascarán isotopic ENSO signal is not forced directly by Pacific SSTs. More accurately, the 18-month lee-wave pattern probably develops as a teleconnection response emanating from the Atlantic coast/Amazon region and therefore is subject to the initial 6- to 8-month time lag between the Pacific and the Atlantic. The lack of a strong foreshadowing isotopic signature in Andean snowfall is also an interesting result in light of the "canonical" warm event development that is thought to be preceded by unusually strong trade wind circulation in the "antecedent" phase [*Rasmusson and Carpenter*, 1982]. It might be expected to see evidence of this tendency in the Huascarán record, as tropical South America remains in a strong trade wind regime throughout the year. However, there is only a moderate response in the year before the zero point, which is overshadowed by the much more significant trailing effect at roughly +12 months.

El Niño events that peak in the first half of the calendar year (coincident with the wet season in Amazonia) exhibit a large Atlantic sector influence in the peak phase, as evidenced by the strong enrichment in the HSC2 $\delta^{18}O$ SEA results. The lack of a similar response for late-peaking El Niños may be due to either/both (1) the reduced Andean snowfall amounts during the period surrounding the peak months of many late events (i.e., August-October) may not allow the signal to be sufficiently recorded and archived and (2) the strong dry winds dominant in the midtroposphere in the late season months (again August-October) may not provide the proper environment for strong linkage between surface conditions and those aloft (e.g., the 500 hPa circulation). Furthermore, a recent study [*Uvo et al.*, 1998] of the relationships between the tropical Pacific SSTs and the precipitation patterns in northeast Brazil indicated particularly strong correlations in the late wet season (April-May). As every moderate-strong El Niño peaking between January and July is likely to display strong warming in these two months that demonstrate close interaction, this seasonal contrast is not unexpected.

On the multiannual scale (Figure 5), there is some evidence that the enrichment of ^{18}O in Huascarán precipitation occurs during some combination of warmer continental temperatures and reduced precipitation in Amazonia. Temperature changes at 500 hPa over tropical South America are concomitant with variations in surface temperature and atmospheric thickness, as the amount of surface heating regulates the height of the tropopause and the height of constant pressure levels in between. Over the 25-year period investigated, the largest fluctuations in temperature/thickness have been ENSO-related, apart from the upward shift to warmer conditions occurring from 1975 to 1978. Several of these warm episodes are coincident with periods of enriched $\delta^{18}O$ in HSC2, particularly noticeable in 1983. Also, an upward shift (though not unprecedented in the 20th century) to a higher mean isotopic state also occurs in the late 1970s, very similar to the abrupt temperature increase and the related rise in the zero isotherm [*Diaz and Graham*, 1996]. However, because many other features of the temperature profile are not duplicated in the isotopic record, there are certainly other regulating factors that need to be identified.

Following further examination of available information, a linkage between the behavior of the zonal winds and SST distribution can be proposed. *Hastenrath* [1984] demonstrated that a southward shift of the ITCZ enhances the zonal surface trade winds at 10°S. The expected implication for Andean precipitation is an enhanced rain-out depletion via a more pluvial environment within the Amazon Basin (0°-10°S) whenever the N-S AtlSST gradient is negative, and vice versa. Support for the trade-wind concept also comes from an analysis by *Rao et al.* [1993], who showed that the strength of the surface wind vector oriented perpendicular to the coast (i.e., southeasterly) determines the amount of rainfall received along the Atlantic margin of Brazil between 5° and 15°S. The suggestion then of (unidirectional) velocity convergence as a mechanism controlling rainfall along the water vapor transport path to Huascarán could help to explain the linking of zonal wind strength to rain-out depletion of ^{18}O. However, this localized "land breeze" coupled with minor orography in eastern Brazil needs to be integrated with the hydrologic processes of the remainder of the Amazon Basin before any further generalizations are made. Finally, a recent study of meteorological conditions over the Bolivian Altiplano [*Garreaud*, 1999] determined that concentrated zones of active convection occur at the 500 hPa level during anomalously wet periods, augmented by stronger easterly flow in the regional circulation pattern at 500 hPa and above. In addition, *Newell and Zhu* [1994] report the existence of "tropospheric rivers of water vapor" from their analysis of atmospheric specific humidity and wind velocity data. If such filamentary structures in atmospheric water vapor were common phenomena over large areas of the Andean front, there could be a quantifiable relationship derived among upper air circulation, barrier-generated velocity convergence, and high Andean precipitation.

The schematic drawing presented in Figure 6 illustrates a potential teleconnection sequence for a "canonical" El Niño that satisfies the major characteristics of the SEA composites in the top half of Figure 4 and generally agrees with other analyses of ENSO influence on tropical Atlantic conditions and Nordeste precipitation [*Mechoso et al.*, 1990; *Uvo et al.*, 1998]. Following a period of enhanced easterlies over the Atlantic (the antecedent phase) the El Niño sequence begins as a sharp warming along the Peru coast, which is transported to the Atlantic basin via the "atmospheric bridge" (indicated here by a simultaneous/delayed weakening of the trade wind circulation at 20°N and 20°S, respectively). From the resulting wind stress anomalies during the onset phase, southeasterly in the South Atlantic turning southwesterly north of the equator (as in the work of *Chang et al.* [1997]), the classic N-S dipole is produced as a surface ocean response. The presumed continental response is a shift in heavy precipitation from the equatorial region toward the subtropical jets in both hemispheres, a coincident weakening of the 500 hPa easterlies, and enrichment of ^{18}O in Andean snowfall. Eventually, all trade winds relax and the tropical Atlantic (i.e., AtlSST) reaches peak warmth, as the PacSST is already starting to cool.

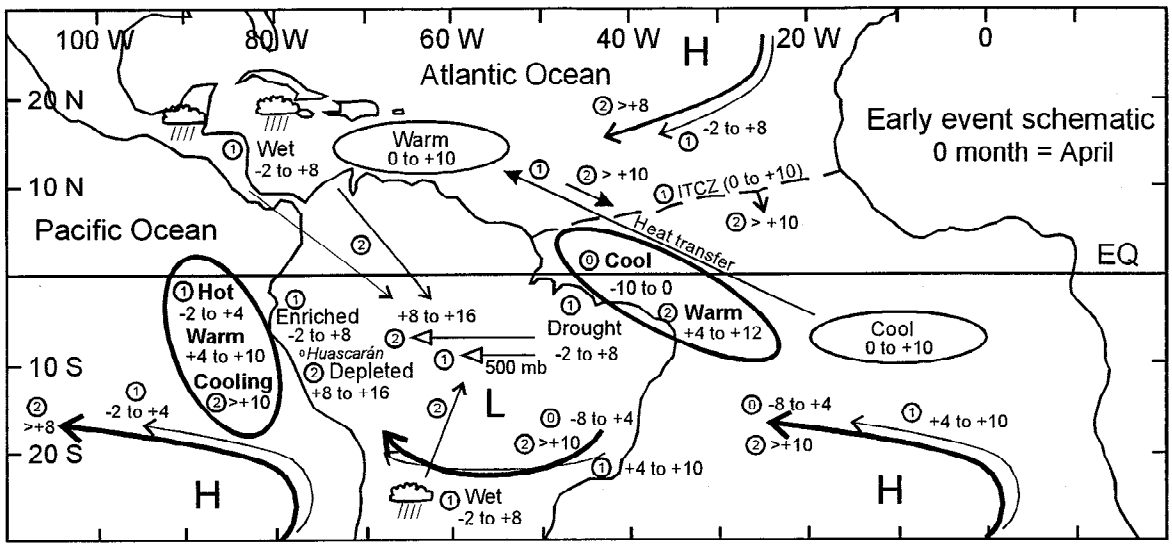

Figure 6. Schematic diagram illustrating the spatial and temporal relationships potentially responsible for the characteristic response of Huascarán isotopic composition to the growth and decay of early-peaking El Niños in the eastern equatorial Pacific. The following terms are used to characterize the various responses: for SST's (cool, warm, hot), for precipitation (wet, normal, drought), and for HSC2 isotopic composition (enriched, depleted). Circled numbers refer generally to (0) antecedent phase, (1) onset-peak phase, (2) decay and post-ENSO phase. Months (plus and minus) indicated are relative to the SEA zero month, as identified by the peak PacSST warming. (Arrows depicting 500 hPa winds are merely symbolic of relative strength, not true anomalies.)

As El Niño reaches maturity, the easterly trades over the Atlantic strengthen such that coastal and equatorial upwelling again brings cooler water to both sides of the equator. The ITCZ, which had been deflected northward following the dipole shift, returns to its normal southerly position (about 5°N) and returns rainy conditions to Amazonia and therefore depleted snowfall to Huascarán. The large magnitude of the post-El Niño depletion (evident in both early and late composites) suggests that unusually strong easterlies and high precipitation often follow the demise of any strong warm event.

Recent interest in tropical Atlantic variability on interannual to decadal scales has been driven by implications for the prediction of hazardous climate anomalies (e.g., ENSO, hurricanes) in North and South America and Africa. Modeling studies and analyses of observational data have produced mechanisms for the teleconnection of SST (and related) anomalies and coastal precipitation patterns. However, for future use of Andean ice core $\delta^{18}O$ data as a proxy for basinscale hydrologic processes, improved understanding of the physical mechanism linking Atlantic SST patterns (i.e., dipole behavior) to the 500 hPa zonal flow over South America needs to be generated. In turn, the lone relationship of these time-averaged zonal winds to Huascarán $\delta^{18}O$ at the expense of temperature and humidity parameters also lacks immediate comprehension. At present, other high-resolution Andean ice cores are being analyzed, and the potential remains that these records may provide important insight into ENSO teleconnections and/or act to extend our knowledge of ENSO variability back into the more distant past. Hence studies focused on these particular problems seem warranted.

5. Summary

The 68-year time series of $\delta^{18}O$ from the Huascarán ice cores is a well-preserved, subannually resolved archive of the environmental conditions over Amazonia and the tropical Atlantic. However, the interannual variations are not an unmodified signal of either oceanic or atmospheric temperatures, only appearing to relate closely to the zonal wind variations over tropical South America at the 500 hPa level. By association (e.g., the similarity in decadal cycles), there is a likelihood that the spatial distribution of temperature anomalies in the tropical Atlantic has influence on the 500 hPa circulation and hence the resultant isotopic composition of propagating moisture. Also, it is probable that enrichment of ^{18}O in Andean snow is related to a combination of warmer atmospheric temperatures and less pluvial conditions but in an uncertain manner. On centennial and longer timescales the temperature control on isotopic composition begins to outweigh the competing effects of precipitation.

The event-based analysis, involving the superposition of individual warm (El Niño) and cold epochs, depicts the typical reaction of the Atlantic-driven tropical engine over Amazonia, through identifying a characteristic 10-14 month half-period $\delta^{18}O$ wave in the composites. During an El Niño the onset of the disturbance occurs precisely at the peak positive anomaly in Pacific sea surface temperature, identifiable by the development of strong enrichment of ^{18}O (significant at the 5% level) soon afterward, and then a full reversal to strongly depleted isotopes 10-14 months afterward. The characteristics of the cold event composites are very similar but opposite, resulting in a very strong negative correlation between warm and cold event composites in the year following peak anomaly development. In the case of El Niño, ^{18}O enrichment associated with the Nordeste drought is most significant when the peak Pacific warming occurs during the first half of the calendar year, coincident with the wet season over Amazonia.

Acknowledgments. We wish to thank Mary E. Davis, Paul Kinder, Bruce Koci, Vladimir Mikhalenko, Cesar Portocarrero, Willie Tamayo Alegre, Selio Villón, and the team of mountain guides, porters, cooks, and arrierros whose assistance in the field logistics were essential. We also thank Chung-Chieh Wang of the OSU Department of Geography for assistance in computer programming and Steve Worley of NCAR for

access to the COADS data. We also gratefully acknowledge Juerg Beer of the Swiss Federal Institute for Environmental Science and Technology, who conducted the accelerator mass spectrometry measurements of ^{36}Cl on the ice core. We also thank Ellen Mosley-Thompson, Gunter Faure, and two anonymous reviewers for their comments and critical review. This research was supported under the NOAA (National Oceanic and Atmospheric Administration) Office of Global Programs (OGP) award, "High Resolution Analysis and Paleoclimatic Interpretation of Ice Cores from the Cordillera Blanca, Peru, Phase III" (Lonnie G. Thompson, principal investigator). Special thanks go to former NOAA-OGP Program Manager David Goodrich and Mark Eakin for their efforts in supporting ice core research in the Andes. This is contribution 1154 of the Byrd Polar Research Center.

References

Bjerknes, J., Atmospheric teleconnections from the equatorial Pacific, *Mon. WeatherRev., 97*, 163-172, 1969.

Bradley, R.S., H.F. Diaz, G.N. Kiladis, and J.K. Eischeid, ENSO signal in continental temperature and precipitation records, *Nature, 327*, 497-501, 1987.

Carter, M.W., and A.A. Moghissi, Three decades of nuclear testing, *Health Phys., 33* (7), 55-71, 1977.

Carton, J.A., X. Cao, B.S. Giese, and A.M. da Silva, Decadal and interannual SST variability in the tropical Atlantic Ocean, *J. Phys. Oceanogr, 26*, 1165-1175, 1996.

Chang, P., L. Ji, and H. Li, A decadal climate variation in the tropical Atlantic Ocean from thermodynamic air-sea interactions, *Nature, 385*, 516-518, 1997.

Craig, H., Isotopic standards for carbon and oxygen and correction factors for mass spectrometric analysis of carbon dioxide, *Geochim. Cosmochim. Acta, 12*, 133-149, 1957.

Cuffey, K.M., G.D. Clow, R.B. Alley, M. Stuvier, E.D. Waddington, and R.W. Saltus, Large arctic temperature change at the Wisconsin-Holocene glacial transition, *Science, 270*, 455-458, 1995.

Dansgaard, W., S. Johnsen, H.B. Clausen, and N. Gundestrup, Stable isotope glaciology, *Meddelelser Grønl., 192* (2), 1-53, 1973.

Diaz, H.F., and N.E. Graham, Recent changes in tropical freezing heights and the role of sea surface temperature, *Nature, 383*, 152-155, 1996.

Enfield, D.B., El Niño, past and present, *Rev. Geophys., 27* (1), 159-187, 1989.

Folland, C.K., and D.E. Parker, Correction of instrumental biases in historical sea surface temperature data, *Q. J. Meteorol. Soc., 121*, 319-367, 1995.

Garreaud, R.D., Multiscale analysis of the summertime precipitation over the Central Andes, *Mon. Weather Rev.*, 127, 901-921, 1999.

Grootes, P.M., M. Stuiver, L.G. Thompson, and E. Mosley-Thompson, Oxygen isotope changes in tropical ice, Quelccaya, Peru, *J. Geophys. Res., 94*, 1187-1194, 1989.

Hammer, C.U., H.B. Clausen, W. Dansgaard, N. Gundestrup, S.J. Johnsen, and N. Reeh, Dating of Greenland ice cores by flow models, isotopes, volcanic debris and continental dust, *J. Glaciol., 20* (82), 3-26, 1978.

Hastenrath, S., On modes of tropical circulation and climate anomalies, *J. Atmos. Sci., 35*, 2222-2231, 1978.

Hastenrath, S., Interannual variability and annual cycle: Mechanisms of circulation and climate in the tropical Atlantic sector, *Mon. Weather Rev., 112*, 1097-1107, 1984.

Henderson, K.A., The El Niño-Southern Oscillation and other modes of interannual tropical climate variability as recorded in ice cores from the Nevado Huascarán col, Peru, M.S. thesis, Ohio State Univ., Columbus, 1996.

Houghton R.W., and Y.M. Tourre, Characteristics of low-frequency sea surface temperature fluctuations in the tropical Atlantic, *J. Climate, 5*, 765-771, 1992.

Johnsen, S.J., W. Dansgaard, and J.C. White, The origin of Arctic precipitation under present and glacial conditions, *Tellus, ser. B, 41*, 452-468, 1989.

Johnson, A.M., The climate of Peru, Bolivia, and Ecuador, in *World Survey of Climatology*, vol. 12, *Climates of Central and South America*, edited by W. Schwerdtfegler, pp. 147-218, Elsevier, New York, 1976.

Jouzel, J., Isotopes in cloud physics: Multiphase and multistage condensation processes, in *Handbook of Environmental Isotope Geochemistry*, vol. 2, *The Terrestrial Environment, B*, edited by P. Fritz and J.C. Fontes, pp. 61-112, Elsevier, New York, 1986.

Kaplan, A., M.A. Cane, Y. Kushnir, A.C. Clement, M.B. Blumenthal, and B. Rajagoplan, Analyses of global sea surface temperature 1856-1991, *J. Geophys. Res., 103*, 18,567-18,589, 1998.

Klein, S.A., B.J. Soden, and N.-C. Lau, Remote sea surface temperature variations during ENSO: Evidence for a tropical atmospheric bridge, *J. Climate, 12*, 917-932, 1999.

Mechoso, C.R., S.W. Lyons, and J.A. Spahr, The impact of sea surface temperature anomalies on the rainfall over northeast Brazil, *J. Climate, 3*, 812-826, 1990.

Mehta, V.M., Variability of the tropical ocean surface temperatures at decadal-multidecadal timescales, part I, The Atlantic Ocean, *J. Climate, 11*, 2351-2375, 1998.

Mehta, V.M., and T. Delworth, Decadal variability of the tropical Atlantic Ocean surface temperature in shipboard measurements and in a global ocean-atmosphere model, *J. Climate, 8*, 172-190, 1995.

Moura, A.D., and J. Shukla, On the dynamics of droughts in northeast Brazil: Observations, theory and numerical experiments with a general circulation model, *J. Atmos. Sci., 38*, 2653-2675, 1981.

Newell, R.E., and Y. Zhu, Tropospheric rivers: A one-year record and possible application to ice core data, *Geophys. Res. Lett., 21*(2), 113–116, 1994.

Quinn, W.H., The Large-scale ENSO event, the El Niño and other important regional patterns, *Bull. Inst. Franç. Étud. Andines, 22* (1), 13-34, 1993.

Quispe Arce, J., Variaciones de la temperatura superficial del mar en Puerto Chicama y del Índice de Oscilación del Sur: 1925-1992, *Bull. Inst. Franç. Étud. Andines, 22* (1), 111-124, 1993.

Rao, V.B., M.C. deLima, and S.H. Franchito, Seasonal and interannual variations of rainfall over eastern northeast Brazil, *J. Climate, 6*, 1754-1763, 1993.

Rasmusson, E.M., and T.H. Carpenter, Variations in tropical sea surface temperature and surface wind fields associated with the Southern Oscillation/El Niño, *Mon. Weather Rev., 110* (5), 354-384, 1982.

Rozanski, K.S., S. Johnsen, U. Schotterer, and L.G. Thompson, Reconstruction of past climates from stable isotope records of palaeo-precipitation preserved in continental archives, *Hydrol. Sci. J. Sci. Hydrol., 42* (5), 725–745, 1997.

Servain, J., Simple climate indices for the tropical Atlantic Ocean and some applications, *J. Geophys. Res., 96*, C8, 15,137-15,146, 1991.

Synal, H.-A., J. Beer, U. Schotterer, M. Suter, and L.G. Thompson, Bomb-produced ^{36}Cl in ice core samples from mountain glaciers, in *Glaciers From the Alps: Climate and Environmental Archives*, pp. 99-102, Paul Scherrer Inst., Villigen, Switzerland, 1997.

Thompson, L.G., Analysis of the concentration of microparticles in an ice core from Byrd Station, Antarctica, *Tech. Rep. 46*, 43 pp., Inst.of Polar Stud., Ohio State Univ., Columbus, 1973.

Thompson, L.G., Ice core evidence from Peru and China, in *Climate since A.D. 1500*, edited by R.S. Bradley and P.D. Jones, pp. 517-548, Routledge, New York, 1992.

Thompson, L.G., E. Mosley-Thompson, P.M. Grootes, M. Pourchet, and S. Hastenrath, Tropical Glaciers: Potential for ice core paleoclimatic reconstructions, *J. Geophys. Res., 89*, 4638-4646, 1984a.

Thompson, L.G., E. Mosley-Thompson, and B. Morales Arnao, El Niño-Southern Oscillation events recorded in the stratigraphy of the tropical Quelccaya Ice Cap, Peru, *Science, 226*, 50-53, 1984b.

Thompson, L.G., E. Mosley-Thompson, M.E. Davis, P.-N. Lin, T. Yao, M. Dyurgerov, and J. Dai, "Recent warming": Ice core evidence from tropical ice cores with emphasis on Central Asia, *Global Planet. Changes, 7*, 145-156, 1993.

Thompson, L.G., E. Mosley-Thompson, M.E. Davis, P.-N. Lin, K.A. Henderson, J. Cole-Dai, J.F. Bolzan, and K.-b. Liu, Late glacial stage and Holocene tropical ice core records from Huascarán, Peru, *Science, 269*, 46-50, 1995.

Thompson, L.G., et al., A 25,000-year tropical climate history from Bolivian ice cores, *Science, 282*, 1858-1864, 1998.

Uvo, C.B., C.A. Repelli, S.E. Zebiak, and Y. Kushnir, The relationships between tropical Pacific and Atlantic SST and Northeast Brazil monthly precipitation, *J. Climate, 11*, 551-562, 1998.

Vautard, R., P. Yiou, and M. Ghil, Singular-spectrum analysis: A toolkit for short, noisy chaotic signals, *Physica D, 58*, 95-162, 1992.

Vuille, M., D.R. Hardy, C. Braun, F. Keimig, and R.S. Bradley, Atmospheric circulation anomalies associated with 1996/1997 summer precipitation events on Sajama Ice Cap, Bolivia, *J. Geophys. Res., 103*, 11,191-11,204, 1998.

Wallace, J.M, E.M. Rasmusson, T.P. Mitchell, V.E. Kousky, E.S., Sarachik, and H. von Stroch, On the structure and evolution of ENSO-related climate variability in the tropical Pacific: Lessons from TOGA, *J. Geophys. Res., 103*, 14,242-24,259, 1998.

Webster, P. J., The large-scale structure of the tropical atmosphere, in *Large-Scale Dynamic Processes in the Atmosphere*, edited by B. J. Hoskins and R. Pierce, pp. 235-276, Academic, New York, 1983.

Woodruff, S.D., R.J. Slutz, R.L. Jenne, and P.M. Steurer, A comprehensive ocean-atmosphere data set, *Bull. Am. Meteorol. Soc., 68* (10), 1239-1250, 1987.

Xie, S.-P., A dynamic ocean-atmosphere model of the tropical Atlantic decadal variability, *J. Climate, 12*, 64-70, 1999.

Yao, T., L.G. Thompson, E. Mosley-Thompson, Y. Zhihong, X. Zhang, and P.-N. Lin, Climatological significance of $\delta^{18}O$ in north Tibetan ice cores, *J. Geophys. Res., 101*, 29,531-29,537, 1996.

K. A. Henderson, L. G. Thompson, and P.-N. Lin, Byrd Polar Research Center, Ohio State University, 108 Scott Hall, 1090 Carmack Road, Columbus, OH, 43210-1002. (henderson.120@osu.edu).

(Received February 5, 1999; revised September 3, 1999; accepted September 9, 1999)